觀察一維紊流數據的一種有效之新拆解法

A New and Effective Tool to Look into Details of a Turbulent Data String

Yih-Nen Jeng, Professor
Department of Aeronautics and Astronautics
National Cheng-Kung University, Tainan, Taiwan, 70101
Email: Z6208016@email.ncku.edu.tw
Chi-Tsung Chen, Ph.D Candidate
Department of Aeronautics and Astronautics
National Cheng-Kung University
You-Chi Cheng
No. 111, Tongpin Rd. Tainan, Taiwan

ABSTRACT

The continuous wavelet (Morlet) transform is modified by adding a Gaussian window to the Fourier spectrum corresponding to the scale function. The Jeng and Cheng strategy of effectively suppressing the non-periodic and low frequency error of the spectrum together with an iterative filter are employed so that the windowing procedure on the spectrum domain can be accurately done. The existence of the inverse transform of the present modified transformation can be shown. The bandwidth of the resulting two-dimensional wavelet coefficient plot of a single sine function is much narrower than that generated by the original Morlet transform. Subsequently, the visibility of the wavelet coefficient plot of several waves with frequencies closing to each other is significantly improved. The application of the proposed wavelet transform to the velocity data string of a low speed turbulent wake flow after a blunt body clearly shows many details which are not known before. On the resulting wavelet coefficient plots, many frequency splitting and merging procedures between waves can be easily captured. The data shows that an energy cascade process is not a simple frequency transformation. It involves a sequence of frequency splitting and merging. The results also show that a systemic and intensive restudy upon a turbulent flow field is necessary to explain the physical meaning of all the detailed insights of a turbulent flow data.

Keywords: New tool of detailed turbulent information, modified Morlet transform, Gaussian window on spectrum domain, spectrum without low frequency error.

Introduction

The study upon a turbulent flow field is seriously restricted by the fact that there is not effective tool to look into the details. In spite of the fact that many turbulent data can be easily and effectively collected, people can only calculate the overall Fourier spectrum, turbulent kinetic energy, and a few other lumped properties. Together with results of the Direction Numerical Simulation (DNS) and flow visualization, people do grasp many physical insights. However, precise interpretation of the effect of numerical error upon a DNS data is still an open and difficult issue. The development of flow visualization is still far away from the stage of clearly providing detailed information of a turbulent flow field. As a consequence, people can only understand a turbulent flow field to a limited extend.

As the continuous wavelet transform was introduced to study turbulent flow [1-4], many studies followed up [5-12] because they agreed with the view point of Farge that the Morlet transform can provide the local information of spectrum. In Ref.[2,3] Farge also pointed that the Fourier spectrum reflects the lumped information over the expansion range and can not provide the local information. Unfortunately, there are not much detailed information can be directly obtained from the resulting wavelet coefficient plot. Therefore, people have to employ other techniques to extract desired information from the resulting wavelet coefficient plot.

Recently, there were two studies [13,14] were related to the drawbacks of the continuous wavelet transform. In Ref.[13], the factors inducing the low frequency error of a Fourier spectrum was identified to be: non-periodic condition, non-periodic part of the data string, and insufficient expansion range of the long wave part. Therefore, the low frequency error was fixed so that one can obtain a spectrum with the error in the order of a high order non-oscillatory interpolation's error. However, a later study [14] showed that the method of removing the non-periodic and long wave parts of a data string is not perfect. An iterative high passed filter was then proposed.

In this study, the non-periodic and long wave parts of a data string are removed by the iterative filter of Ref.[14] and an accurate Fourier spectrum is then obtained by the strategy of Ref.[13]. With an correct Fourier spectrum in hand, the Morlet transform can then be re-manipulated successfully as the present study done.

Analysis

For the sake of completeness, the works of Ref.[13,14] are briefly reviewed. In Ref.[13], the following strategy was proposed:

1. Choose zero crossing points at two ends. Use an interpolation method to find 0 points there.
2. Use the monotonic cubic interpolation of Ref.[15] to regenerate the data so that total number of points are of 2^m. Note that more than one point should be located in the range between two successive data points of the original data string to reduce interpolation error.
3. A simple and fast Fourier sine transform algorithm is employed to generate the desired spectrum.

Because the zero values at two ends are used and the Fourier sine transform is employed, no any error due to non-periodic condition is introduced except the interpolation error. Since the values are chosen at two ends, the penalty of shrinking the available data range can not be avoided.

Assume that a discrete data string can be approximated by

$$y(t) = \sum_{n=0}^{N} b_n \cos\left(\frac{2\pi t}{\lambda_n}\right) + c_n \sin\left(\frac{2\pi t}{\lambda_n}\right) \qquad (1)$$

In Ref.[14], it was proven that after applying the Gaussian smoothing once, the resulting smoothed data becomes

$$\bar{y}_1(t) \approx \sum_{n=0}^{N} a(\sigma/\lambda_n)\{b_n \cos\left(\frac{2\pi t}{\lambda_n}\right) + c_n \sin\left(\frac{2\pi t}{\lambda_n}\right)\} \qquad (2)$$

where $a(\sigma/\lambda_n)$ is the attenuation factor introduced by the smoothing and can be proven numerically that

$$0 \le a(\sigma/\lambda_n) \approx \exp[-2\pi^2\sigma^2/\lambda_n^2] \le 1 \qquad (3)$$

If the removed high frequency part is denoted as y_1' and apply the same smoothing to it to obtain the second smoothed result as $\bar{y}_2$ and repeat the same procedure to obtain the $m-$th smoothed and high frequency part as $\bar{y}_m$ and y_m', respectively. The following relation can be built

$$y_m' = \sum_{n=0}^{N} [1-a(\sigma/\lambda_n)]^m \left[b_n \cos\left(\frac{2\pi t}{\lambda_n}\right) + c_n \sin\left(\frac{2\pi t}{\lambda_n}\right)\right]$$

$$\bar{y}(m) = \bar{y}_1 + \bar{y}_2 + \ldots + \bar{y}_m =$$

$$= \sum_{n=0}^{N} \{1-[1-a(\sigma/\lambda_n)]^m\} \left[b_n \cos\left(\frac{2\pi t}{\lambda_n}\right) + c_n \sin\left(\frac{2\pi t}{\lambda_n}\right)\right] \qquad (4)$$

$\bar{y}(m)$ can be considered as the smoothed part and y_m' as the high frequency part. It was proven in Ref.[14] that the transition region from $\{1-[1-a(\sigma/\lambda_n)]^m\}$ = 0 to 1 is much narrower than that of the original $a(\sigma/\lambda_n)$.

The following Morlet transform transfer a data string $y(t)$ into the wavelet coefficient.

$$W(a,\tau) = \frac{1}{\sqrt{a}} \int_{-\infty}^{\infty} y(x)\psi^*(\frac{x-\tau}{a})dx \qquad (5)$$

where $\psi(x) = e^{i6x}e^{-|x|^2/2}$ and a is called as the scale function. If this transform is applied over a range

$a_0 \le a \le a_1$, a two-dimensional wavelet coefficient plot is obtained on the (a,τ) plane. By applying Eq.(5) to Eq.(1), it can be easily shown that, the resulting equation can be approximated by

$$W(a,\tau) \approx \sum_{n=0}^{N} b_n \sqrt{\frac{\pi a}{2}} \exp\left(-\frac{a^2}{2}\left(\frac{2\pi}{\lambda_n}-\frac{6}{a}\right)^2\right)\left[\cos\frac{2\pi\tau}{\lambda_n}+i\sin\frac{2\pi\tau}{\lambda_n}\right] + \sum_{n=0}^{N} c_n \sqrt{\frac{\pi a}{2}} \exp\left(-\frac{a^2}{2}\left(\frac{2\pi}{\lambda_n}-\frac{6}{a}\right)^2\right)\left[\sin\frac{2\pi\tau}{\lambda_n}-i\cos\frac{2\pi\tau}{\lambda_n}\right] \quad (6)$$

A careful inspection upon this formula reveals that, if the original data is of the form

$$y(t) = \sin\left(\frac{2\pi t}{\lambda_m}\right), \quad t_1 < t < t_2 \qquad = 0 \quad \text{otherwise} \quad (7)$$

where $\lambda_m = a\pi/3$, the response of Eq.(6) will give a non-zero value in the region of $t_1 - 6.5a < t < t_2 + 6.5a$ and $0.65\lambda_m < \lambda < 2.4\lambda_m$. Since the wavelet coefficient changes with respect to the scale function a, one can not further improve this contaminated region on the time domain. However, the contaminated region on the frequency domain can be improved by adding a window to the original data say

$$y(t) = \sum_{n=0}^{N}\left\{b_n \cos\left(\frac{2\pi t}{\lambda_n}\right) + c_n \sin\left(\frac{2\pi t}{\lambda_n}\right)\right\} \exp[-\frac{(f_m - f_n)}{2\sigma^2}] \quad (8)$$

where $f_m = T/\lambda_m$, $f_n = T/\lambda_n$ and T is the data range in time domain. This windowing procedure can be effectively achieved only if the spectrum is accurately evaluated. The resulting wavelet coefficient takes the form

$$\overline{W}(a,\tau,y) \approx \sqrt{\frac{\pi a}{2}} \times \left\{\sum_{n=0}^{\infty} b_n \exp\left(-\frac{a^2}{2}\left(\frac{2\pi}{\lambda_n}-\frac{6}{a}\right)^2 - \frac{[n-3T/(a\pi)]^2}{2\sigma^2}\right)\exp\left[\frac{i2\pi\tau}{\lambda_n}\right] + \sum_{n=0}^{\infty} c_n \exp\left(-\frac{a^2}{2}\left(\frac{2\pi}{\lambda_n}-\frac{6}{a}\right)^2 - \frac{[n-3T/(a\pi)]^2}{2\sigma^2}\right)\exp\left[-\frac{i2\pi\tau}{\lambda_n}\right]\right\} \quad (9),$$

where n is the mode number corresponding to f_n and λ_n and $\lambda_m = a\pi/3$. If one perform the summation over all the values of a's, the inverse transform can be easily obtained from the real part because the factor embedded to the spectrum b_n and c_n in Eq.(9) are the same.

In order to effectively reflect the original data's character, let

$$k_{n-1} = T/\lambda_{n-1},\ k_n = T/\lambda_n,\ k_{n+1} = T/\lambda_{n+1} \quad (10)$$

The window size scale σ takes the following value

$$\sigma = c \cdot \max[|k_n - k_{n-1}|, |k_{n+1} - k_n|] \quad (11)$$

where $c = 1$ or 2 is employed in this study.

Results and Discussions

Figure 1a is the wavelet coefficient plot of the following function generated by the original Morlet transform, say

$$y(x) = \sin(2\pi f x)$$
$$f = 4, \quad x \le 8$$
$$= 4 + (x-8)/4, \quad 8 < x < 12$$
$$= 5, \quad 12 \le x \quad (12)$$

That shown in Fig.1b is the result of present modification with $c = 1$. It is seen that the resolution of the present modification is significant. However, the frequency variation can not be captured very well which is caused by the Gaussian kernel function. If two waves $\sin(8.7\pi x)$ and $\sin(9.3\pi x)$ are added the original Morlet transform cannot reflect these three waves but the present modification gives the result shown in Fig.2 where three waves can be easily distinguished.

Now the experimental data of Ref.[10] is employed to demonstrate the present modified wavelet transform. The u velocity data at $0.5d$ and $3d$ downstream locations along the centerline of the blunt body's wake region are examined (see Fig.3a), respectively, where $d = 32$mm is the width of the blunt body and Re_d =16500 is employed. The location of $0.5d$ is within the wake region, while that of $3d$ is at the down stream side out of the wake. The removed smoothed part corresponding to these two data string is shown in Fig.3b and 3c, respectively. It is obviously that if these parts are not removed, the corresponding spectrums will involve their contribution over the whole spectrum domain which introduces certain error. The resulting spectrums are shown in left and right of Fig.4, respectively. From these spectrums, it is obviously that at

$0.5d$ location, there is not obvious shedding frequency mode. On the other hand, at $3d$ location, the dominate and three sub-harmonic modes can be easily captured. Note that, if their non-periodic parts are not removed, the second and third the sub-harmonic modes can not be easily captured. Generally, the third mode might be ignored because it is interfered by the low frequency error.

The wavelet coefficient plots corresponding to $0.5d$ and $3d$ are shown in Fig.5 and Fig.6, respectively. Both the energy (amplitude) and real part of Fig.5 show that the vortex shedding information $x = 0.5d$ presents in a piecewise manner which can be seen along the line of $a = 0.0133$ (≈ 72 Hz and $\mathrm{St} = fd/U_0 = 0.305$). Many sub-harmonic modes also present in the same piecewise manner. Moreover, the frequency splitting and merging can be seen here and there between these dominate and sub-harmonic modes. It seems that from the real part plot one can get a more direct feeling upon the feature than that of the amplitude plot because the phase information give us a direction impression about the flow oscillation. The result shown in Fig.6 reflects that the vortex shedding does not give a perfect continuous spectrum line around the $a = 0.0133$ line. This is true because a vortex shedding from the inclined surface of the blunt body shown in Fig.3a can not always generate a regular and well structured vortex as can be seen from the flow visualization plot of Ref.[10]. Moreover, the high order sub-harmonic modes can not exactly persist their frequencies at exactly the integer multiples of the dominate frequency, say integer multiples of $a = 0.0133$.

Part of the information of the energy cascade can be found by examining many left and right inclined waves between the dominate and the first sub-harmonic modes of Fig5 and Fig.6, respectively. In Fig.5, the complex structures of these waves between dominate modes show that the energy cascade within the wake region is not a simple path. On the other hand, at the $x = 3d$ location where the mean velocity is almost recovered from small scaled waves, all the small scale waves will be eventually dissipated out. Consequently, one can see many left inclined wave stemming from the first sub-harmonic mode and running toward the first dominate mode and from the first mode toward still more fine scale waves as shown. These left inclined waves are not in a single and straight manner. They also involve many frequency splitting and merging procedure.

Since the experimental facilities does not involve a high speed camera and flow visualization via laser sheet splitting, the flow structure corresponding to all the details of frequency splitting and merging between waves of different wavelengths can not be exactly addressed. It seems that systematic restudies about this and many other turbulent flow fields are necessary so that the physics of the frequency splitting and merging can be correctly captured.

Conclusions

A new and effective tool to inspect a complicated data string of a turbulent flow field was successfully developed by modifying the Morlet transform. The visibility of the resulting wavelet coefficient plot along the frequency direction is significantly recovered by employing an iterative filter and a simple strategy of removing the low frequency error of the Fourier spectrum. Many resulting turbulent flow details on the spectrum domain are first seen so that they can only be partially explained. It seems that systematic and well organized experiments are necessary to obtain a fully understanding about a turbulent flow field. Besides, further developments upon many fields related to complicated data strings can be started by employing the present modifications upon the Fourier spectrum and continuous wavelet transform. A series of study upon brain, neural, and earth quake signals are on the way.

Acknowledgement

The authors acknowledge the support by the National Science Council, Republic of China, for this research under contract NSC-93-2212-E006-037. The experimental data was given by my colleague, Prof. Miau, and is gratefully acknowledged.

Reference

1. A. Grossmann and J. Morlet, “Decomposition of Hardy Functions into Square Integrable Wavelets of Constant Shape,” SIAM J. Math. Anal. Vol.15 no.4, July 1984.

2. M. Farge, “Wavelet Transforms and Their Applications to Turbulence,” Annu. Rev. Fluid Mech., vol.24, pp.395-457, 1992.
3. M. Farge, N. Kevlahan, V. Perrier, and E. Goirand, “Wavelts and Turbulence,” Proc. IEEE, vol.84, no.4, pp.639-669, April 1996.
4. B.Ph. van Milligen, E. Sanchez, T. Estrada, C. Hidalgo, and B. Branas, “Wavelet Bicoherence: A New Turbulence Analysis Tool,” Phys. Plasmas vol.2, no.8, pp.1-35, Aug. 1995. 3017.
5. V. Tarasov, E. Dubinin, S. Perraut, A. Roux, K. Sauer, A. Skalsky, and M. Delva, “Wavelet Application to the Magnetic Field Turbulence in the Upstream Region of the Martian Bow Shock,” Earth Planets Space, vol.50, p.699-708, 1998.
6. G. Buresti, G. Lombardi, and J. Bellazzini, “On the Analysis of Fluctuating Velocity Signals through Methods Based on the Wavelet and Hilbert Transforms,” Chaos Solitons & Fractals, vol.20, pp.149-158, 2004.
7. R. Carmona, W. L. Hwang, and B. Torresani, *Practical Time-Frequency Analysis*, Academic Press, 1998.
8. P. S. Addison, “Wavelet Analysis of the Breakdown of a Pulsed Vortex Flow,” Proc. Instn Mech. Engrs., vol.213 part C, pp.217-229, 1999.
9. Z. Zhang, H. Kwwabata, and Z. Q. Liu, “EEG Analysis Using Fast Wavelet Transform,” Proc. IEEE pp.2959, 2000.
10. C. T. Wang, “Investigation of Low-Frequency Variations Embedded in Vortex Shedding Process,” Ph.D dissertation, Department of Aeronautics and Astronautics, National Cheng-Kung University, June 2000.
11. J. J. Miau, S. J. Wu, C. C. Hu, and J. H. Chou, “Low Frequency Modulations Associated with Vortex Shedding form Flow over Bluff Body,” AIAA J., vol.42, no.7, pp.1388-1397, 2004.
12. S. J. Wu, J. J. Miau, C. C. Hu, and J. H. Chou, “On Low-Frequency Modulations an Three-Dimensionality in Vortex Shedding behind Flat Plates,” J. Fluid Mechanics, vol.526, pp.117-146, 2005.
13. Y. N. Jeng and Y. C. Cheng, “A simple Strategy to Evaluate the Frequency Spectrum of a Time Series Data with Non-Uniform Intervals,” Trans. Aero. Astro. Soc. R. O. C., vol.36, no.3, pp.207-214, 2004.
14. Y., N, Jeng, P. G. Huang, and H. Chen, “Filtering and Decomposition of Waveform in Physical Space Using Iterative Moving Least Squares Methods,” AIAA paper No.2005-1303, 2005.
15. H. T. Huynh, “Accurate Monotone Cubic Interpolation,” *SIAM J. Number. Anal*. vol.30, no.1, pp57-100, Feb.1993.

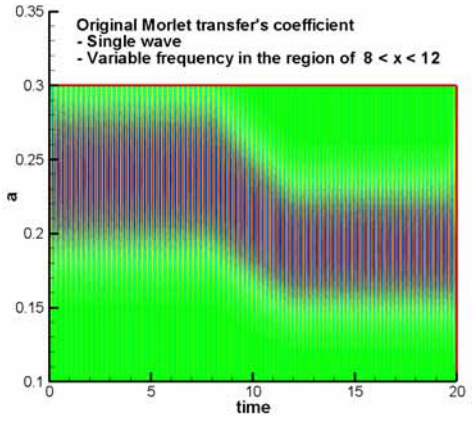

Fig.1a The real part of the wavelet coefficient plot evaluated by the original Morlet transform

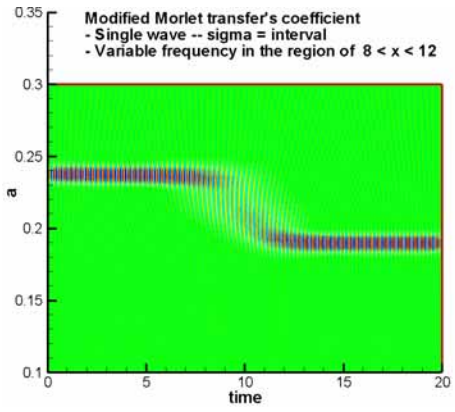

Fig.1b The real part of the wavelet coefficient of the wave with a variable frequency by the present modified Morlet transform with $c = 1$ and 40 uniform spaces to resolve the scale $0.1 \le a \le 0.3$.

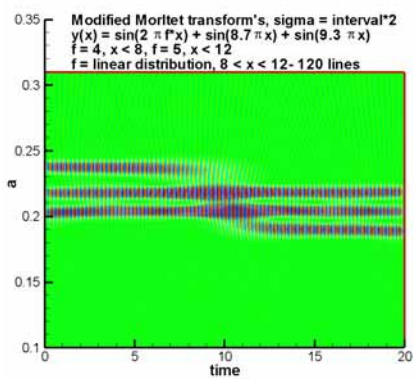

Fig.2 The real part of the wavelet coefficient of a wave with a variable frequency plus two sine waves with fixed frequency by the present modified Morlet transform with $c = 2$ and 120 uniform spaces to resolve the scale $0.1 \le a \le 0.3$.

(3a)

(3b)

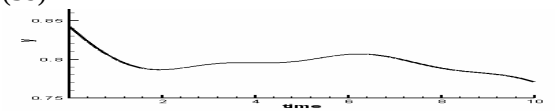

(3c)

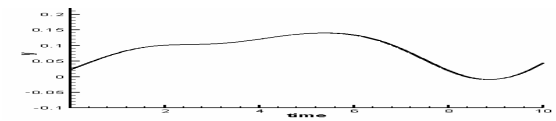

Fig.3 The removed smoothed and non-periodic part of the original data strings at : (3a) schematic diagram; (3b) $x = 0.5d$; and (3c) $x = 3d$, respectively.

(4a)

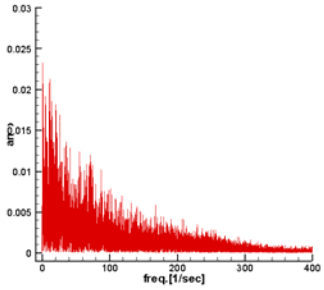

(4b)

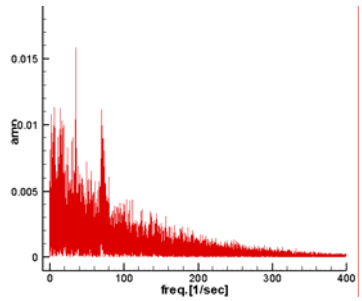

Fig.4 The spectrums corresponding to Fig.3a (4a) and Fig.3b (4b), respectively.

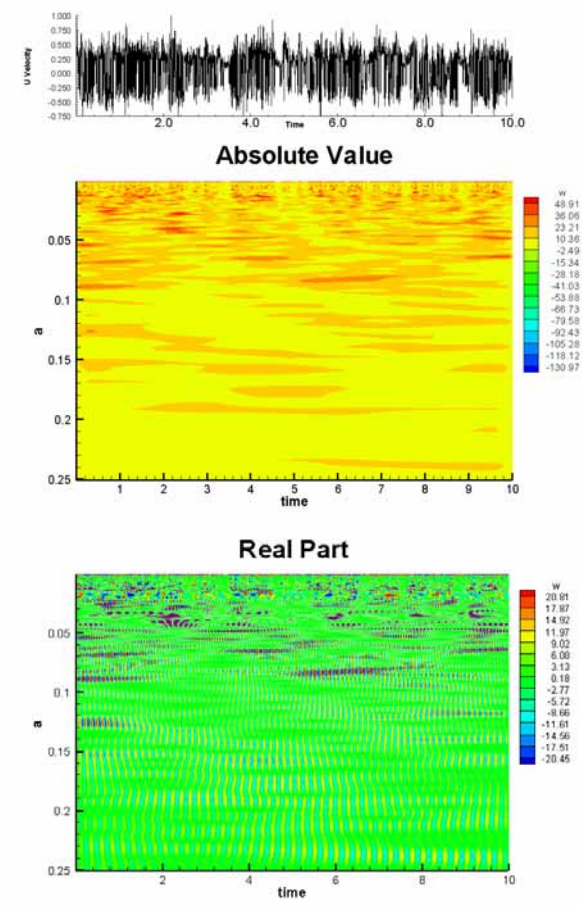

Fig.5 The amplitude and real part of the wavelet coefficient plot of $x = 0.5d$ location, generated by the proposed modified Morlet transform, scale factor of spectrum windowing is $c = 1$.

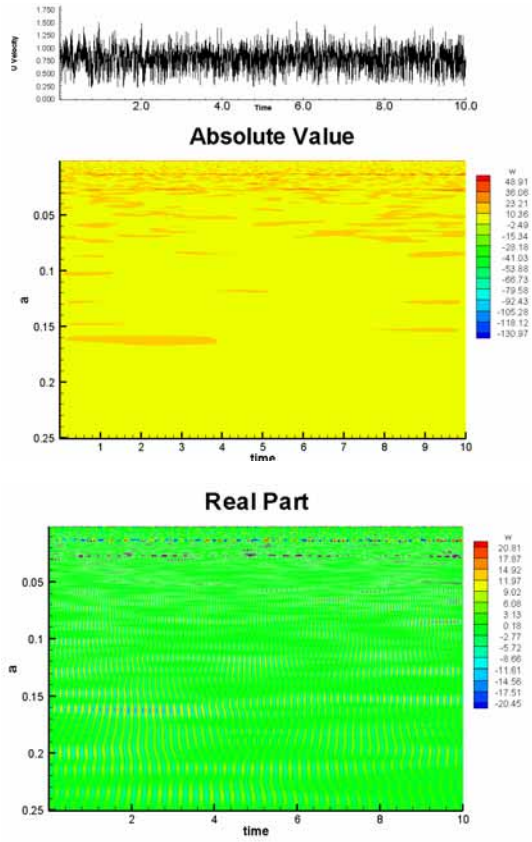

Fig.6 The amplitude and real part of the wavelet coefficient plot at $x = 3d$ location, generated by the proposed modified Morlet transform, scale factor of spectrum windowing is $c = 1$.

觀察一維紊流數據的一種有效之新拆解法

鄭育能 教授
成功大學 航太系
陳季聰
成功大學航太系博士生
鄭又齊
台南市東平路 111 號 5 樓之 5

摘　要

本文改進 Morlet 小波轉換法，使能輕易地看到許多原來各果小波轉換法無法看到的內涵。本文使用 Jeng-Cheng 的簡易 FFT 法則，對數據兩端經內插法取 0 點後，用單調式三次曲線分段內插法重新分佈成均勻點，使點數為 2 的整數次方，要保證原數據間格內至少要有 1 點以上，再對一端取奇函數映射，如此可得到幾乎沒有誤差的正確頻譜。經對頻譜取 Gaussian 窗口式加權法，再作逆 FFT 轉換以得到有限頻寬濾波(band- passed)數據，最後再取 Morlet 轉換。本文的測試例子，說明所得的二為小波係數圖比原方法之結果清析甚多，應用到流經一個鈍頭體的低速紊流之尾流區的速度數據串，發現可以觀測到詳盡的波型變化。

關鍵字：分析紊流數據之新工具，改進之 Morlet 小波轉換法，頻譜之 Gaussian 窗口加權，無低頻誤差頻譜。